

Extraction of information about periodic orbits from scattering functions

T. Bütikofer^a C. Jung^b T.H. Seligman^b

^a*Institut für Physik, Universität Basel, CH-4056 Basel, Switzerland*

^b*Centro de Ciencias Físicas, University of Mexico (UNAM), Cuernavaca, Morelos, Mexico*

Abstract

As a contribution to the inverse scattering problem for classical chaotic systems, we show that we can select sequences of intervals of continuity, each of which yields the information about period, eigenvalue and symmetry of one unstable periodic orbit. PACS: 03.80.+r; 05.45.+b; 94.30.Hn

Key words: chaos; chaotic scattering; inverse scattering problem

In the framework of the study of the inverse scattering problem for classical chaotic scattering in two dimensions, the attention has been focussed on the topology of the chaotic saddle [1,2] and on the definition of an appropriate partition [3]; thermodynamic quantities were also discussed marginally [1]. In none of these approaches the specific properties of the unstable periodic orbits were explicitly searched for. Yet knowledge of these, goes a long way towards understanding the chaotic saddle. Usually the shortest orbits overshadow the chaotic set or, in other words, they form the skeleton of the globally unstable component of the invariant set. As far as semi-classical approximations are concerned, these orbits form the backbone of all considerations that lead to trace formulae [4–6]. The most useful informations are their periods and Lyapunov exponents. These can be used to determine the hierarchical order in the pattern of intervals of continuity (henceforth abbreviated to IOC) in the scattering functions, but at the same time it is this very pattern, which allows us to learn something about the periodic orbits from scattering functions.

In this article we shall focus on the latter part, i.e. on obtaining the periods and the Lyapunov exponents of unstable periodic orbits from regular patterns of the IOC of scattering functions. The latter we define as a function of the points on a line in the space of initial conditions, that gives some property of the scattering process such as e.g. time delay or scattering angle (cf fig. 1).

After recalling some known results [7] concerning the external periodic orbits we present two methods to achieve our goal for periodic orbits that are both fairly short and not too unstable. We illustrate these methods by scattering a charged particle off a magnetic dipole. The reader may want to refer to the figures of the example while reading the description of the general method.

The trajectories belonging to one IOC of a scattering function all leave the interaction region crossing the same external orbit i.e. leaving through the same saddle or “doorway”. When the initial condition approaches one of the boundary points of the IOC from the inside, the scattering trajectory executes an increasing number of revolutions along the saddle orbit before it finally leaves the interaction region. For each revolution we expect an oscillation of the scattering angle (cf fig. 2). The frequency of this oscillations increases with the diverging time delay. An asymptotic observer can determine a sequence of initial conditions from within one and the same IOC, which are separated by a full oscillation of the scattering angle. This sequence converges to the boundary of the IOC in such a way, that, in the limit, the distance from the boundary point decreases by a factor determined by the eigenvalue of the saddle orbit. In the same limit the time delay increases by the period of this orbit, when going from one member of this sequence to the next. From these two quantities the Lyapunov exponent can be calculated. If there are several external orbits we can investigate each of them separately, choosing an appropriate IOC, where the outgoing scattering trajectories cross exactly this orbit before finally leaving the interaction region. Information about any of the internal orbits cannot be obtained in this way.

Based on this result we propose two methods to obtain both periods and Lyapunov exponents for inner periodic orbits. The first will use the time delay function only whereas the second exploits in addition the other scattering functions. To achieve this we analyze how the inner orbits influence the hierarchical pattern of IOC.

The basic idea for our method is provided by the following property of chaotic scattering: To each periodic orbit σ , which can be reached from the outside, there exist infinitely many sequences of IOC (cf fig. 1) of the scattering functions. The common feature of these sequences is the following: As we move along the sequence, sooner or later one step implies precisely one revolution of the trajectory close to the periodic orbit σ . The central problem will be to identify a sequence which is clearly associated with one periodic orbit. If we knew such sequences in advance, then it would be easy to find the period and the Lyapunov exponent of the periodic orbit σ .

We label the IOC forming the selected sequence by $\{I_\sigma^{(k)}\}_{k \in \mathbb{N}}$ where k labels the order of the elements of the sequence, $L(I_\sigma^{(k)})$ indicates the length of the IOC and $t(I_\sigma^{(k)})$ a typical time delay for this IOC which we obtain by choos-

ing a representative trajectory for each IOC. It is convenient to choose the representatives to have the absolute minimal time delay within an IOC.

At large time delays two consecutive representatives differ only in one additional revolution along the unstable periodic orbit. In order to extract periods and Lyapunov exponents of unstable periodic orbits from the time delay function, we need to know the representative time delays and lengths of as many IOC as possible. We determine the ratio $\tilde{\lambda}_\sigma^{(k)} = L(I_\sigma^{(k)})/L(I_\sigma^{(k+1)})$ of the lengths of consecutive pairs of IOC and the difference of their representative time delays $\tilde{T}_\sigma^{(k)} = t(I_\sigma^{(k+1)}) - t(I_\sigma^{(k)})$. We also define

$$\tilde{\Lambda}_\sigma^{(k)} = \frac{1}{\tilde{T}_\sigma^{(k)}} \log(\tilde{\lambda}_\sigma^{(k)}). \quad (1)$$

If the sequence was chosen appropriately, $\tilde{T}_\sigma^{(k)}$ will converge to the period T_σ of the orbit σ , $\tilde{\lambda}_\sigma^{(k)}$ to its eigenvalue λ_σ and $\tilde{\Lambda}_\sigma^{(k)}$ to its Lyapunov exponent Λ_σ .

As mentioned above the choice of the sequence is critical and difficult. We therefore proceed to show how this choice can be partially avoided simultaneously with the approximative evaluation of the quantities above. If we plot either $\tilde{\lambda}_\sigma^{(k)}$ or $\tilde{\Lambda}_\sigma^{(k)}$ against $\tilde{T}_\sigma^{(k)}$ we should find an accumulation point near the correct value of $(\lambda_\sigma, T_\sigma)$ or $(\Lambda_\sigma, T_\sigma)$ respectively. Note that each of the infinitely many sequences associated to one periodic orbit will approach the same accumulation point. Furthermore points $(\tilde{\lambda}_{\sigma'}, \tilde{T}_{\sigma'})$ or $(\tilde{\Lambda}_{\sigma'}, \tilde{T}_{\sigma'})$ erroneously taken because they belong to a sequence for a different periodic orbit will have different accumulation points, except if both period and eigenvalue for the two orbits coincide. If the error is such that the pairs are obtained from IOC of sequences that belong to different periodic orbits no accumulation points are expected. It is thus tempting to perform this plot using points generated for all pairs of IOC available.

In principle we should then find accumulation points for many periodic orbits. This will not be implemented easily because if we have sufficient IOC to expect reasonable convergence along one sequence, the plot would have so many points that it would be very difficult to identify these accumulation points. Even worse, the discrete numerics may simulate structures that do not exist. In order to identify the accumulation points, only pairs of IOC that might belong to the same sequence have to be taken into account. Appropriate strategies to achieve this goal must be developed. An inspection of the hierarchical structure corresponding to the time delay function shows that successive IOC have to be connected by pieces of equal or higher hierarchical order. Therefore only pairs of IOC are tested with no intervening IOC possessing lower time delays. Further filtering may well be necessary.

- If we proceed using the time delay function as the only source of information,

we can start to look for multiplets of IOC which apparently belong to one sequence. Each of its members should have a higher representative time delay than its predecessor without intervening IOC with lower time delays. If such a multiplet belongs to a single sequence its successive IOC should show roughly the same differences in time delay and ratios of successive lengths (cf fig. 3). By narrowing the limits for the allowed differences in time delay and ratios of the multiplets, improved convergence towards a periodic orbit can be promoted.

- If other scattering functions are also available, pairs of IOC that belong to a sequence can be identified by comparing their representative final conditions. Again only pairs of IOC without intervening IOC with lower representative time delays are taken into account. Since the final conditions of representative trajectories converge in the limit of high time delays to a point, two successive IOC can be tentatively identified by looking for those with close representative final conditions.

Both methods yield not only the basic periods but also, in a diminished extent, integer multiples thereof.

To illustrate these methods we use the scattering of a charged point particle off a magnetic dipole. This model is also known as the Störmer problem [8]. After eliminating the rotational degree of freedom and a suitable rescaling in cylindrical coordinates one is left with a Hamiltonian of the form:

$$H(\rho, z) = \frac{1}{2} \left[p_\rho^2 + p_z^2 + \left(\frac{1}{\rho} - \frac{\rho}{\sqrt{\rho^2 + z^2}} \right)^2 \right]. \quad (2)$$

Here (p_ρ, p_z) are the momenta conjugate to (ρ, z) . It is well known that the resulting phase flow represents a chaotic scattering system [9,10]. An analytical proof for its non-integrability is given in [11]. Every scattering trajectory is uniquely determined in the asymptotic region by the impact parameter b_{in} and the angle α_{in} between its velocity vector and the negative ρ -axis. A detailed description of the chaotic dynamics of this system for the energy range $[0.031, 0.081]$ can be found in [10]. The two fundamental periodic orbits of the binary horseshoe will be called A and C . The outer orbit C is accessible from the outside for all energies whereas the inner one A may be at the center of an elliptic island for some energies.

For illustration we will consider the hyperbolic case at an energy $E = 0.062$ and show how to extract information on A and other inner periodic orbits. Note that hyperbolicity is no prerequisite for the methods presented here. For the integration of the equations of motion a Bulirsch-Stoer algorithm [12] has been used. The simulation takes place in a disk of radius 1000 around the origin of the (ρ, z) -plane.

A part of a typical sequence whose trajectories come close to A is shown as

IOC in a time delay function in fig. 1. In fig. 2 the final angles α_{out} of the trajectories from the IOC $\{I_A^{(k)}\}_{1 \leq k \leq 5}$ are plotted against their corresponding time delay values.

In this plot several essential features can be seen.

- (1) As the time delay increases the period of the curves converge towards the period of the outer periodic orbit C . This is a direct consequence of the additional revolutions near C with initial conditions near the boundary of an IOC.
- (2) The differences of the representative (minimal) time delays $t(I_A^{(k)})$ of consecutive IOC converges towards half the period of the inner periodic orbit A .
- (3) The lower end of the curves of every second IOC point in the same direction. This effect has its origin in the common reflection symmetry on the ρ -axis of A and the Hamiltonian. If A and the Hamiltonian had no common symmetry

$$t(I_A^{(k)}) = \frac{1}{2} \left(t(I_A^{(k-1)}) + t(I_A^{(k+1)}) \right) \quad (3)$$

would not be fulfilled. In such a case there would be two sequences whose members were separated by the full period of the corresponding periodic orbit. This shows that by using only the time delay function as a source of information it might be unclear whether we measure the whole period of a periodic orbit without symmetries or its n -th part of an periodic orbit with a cyclic symmetry group of order n . Using additional information provided by other scattering functions as α_{out} and b_{out} can give helpful hints to the answer of this question.

In order to resolve about 608 IOC we scatter 10^7 trajectories with $\alpha_{\text{in}} = 0^\circ$ and b_{in} evenly distributed on the interval $[1.3049, 1.3065]$. If we apply the filter that respects the hierarchical structure and look for triples of IOC $(I_\sigma^{(k-1)}, I_\sigma^{(k)}, I_\sigma^{(k+1)})$ with the property

$$\begin{aligned} \left| \tilde{T}_\sigma^{(k-1)} - \tilde{T}_\sigma^{(k)} \right| &< 0.02 \\ \left| \tilde{\Lambda}_\sigma^{(k-1)} - \tilde{\Lambda}_\sigma^{(k)} \right| &< 0.02 \end{aligned} \quad (4)$$

we end up with 64 of such triples. Each triple of IOC yields two points $(\tilde{\Lambda}^{(k)}, \tilde{T}^{(k)})$ in fig. 3. Not all 128 points are located in the area shown in this figure but the chosen resolution of 10^7 points was too poor for a meaningful prediction of orbits with symmetry reduced periods longer than $T = 15$. The more dots are clustered in a group the likelier it is to find a periodic orbit with roughly these values for its symmetry reduced period and Lyapunov exponent. In fig. 3, apart from the times for one revolution around a symmetry reduced

periodic orbit $(A^{1/2}, C^{1/2})$ integer multiples of these times are also recognizable (A, C) . Among the periodic orbits of our system shown in fig. 4 only three orbits $(A, C$ and $I)$ remain invariant under a reflection on the ρ -axis. The rest of the orbits either change their direction of rotation $(B, D, F, G$ and $H)$ or are mapped onto their mirror image (E) . Thus for orbits A, C and I the half periods show up besides the full ones in fig. 3.

Alternatively we may use pairs with similar final conditions retaining the restriction derived from the hierarchical structure of the time delay function. We accept pairs of IOC whose representative trajectories differ in outgoing angle by less than 0.1° and in the outgoing impact parameter by less than 0.01 in our scale. We plot the 115 obtained points in fig. 5 similar to fig. 3. Now half periods will not appear because we did not symmetrize the outgoing asymptotic parameter. Comparing the two figures we see that the second method allows to identify more periods. While in fig. 3 accumulation points are not very obvious in fig. 5 they appear rather clearly in a few instances. Where they appear the Lyapunov exponent indeed seems to converge toward the exact value. Note the difference in scales for time delay and exponents. Considering that the Lyapunov exponent is an average, once identified, the points belonging to one period can be averaged. Table 1 shows that for the points in fig. 5 the average matches the exact value quite well.

Summarising we have presented a new approach to the inverse scattering problem for chaotic Hamiltonian systems. In distinction to earlier work [1–3] we do not require the system to have an internal or external clock. Furthermore we are able to extract more detailed information about the properties of the most important periodic orbits. The possibilities inherent to this approach are much larger than what was presented in this letter. More extensive research on the filtering techniques must be done and the optimal approach may well depend on the problem. Also much larger numbers of intervals of continuity must be generated to be able to analyze the structure of the $(\tilde{\Lambda}, \tilde{T})$ -plane. Finally the possibility to obtain quite easily the periods of the shortest periodic orbits may be used to provide an inner clock that always exist for the method proposed in [1].

Acknowledgements

The authors wish to thank L. Benet for useful discussions. This work was partially supported by the SNF, the DGAPA (UNAM) project IN-102597 and the CONACYT grant 25192-E. One of the authors (T.B.) wants to thank the CIC for their generous hospitality.

References

- [1] C. Jung, C. Lipp, and T.H. Seligman. The inverse scattering problem for chaotic Hamiltonian systems. *Ann.Phys.*, 275:151, 1999.
- [2] C. Jung, C. Lipp, and T.H. Seligman. Classification of incomplete horseshoes and the chaotic inverse scattering problem. In *Proceedings of the IV Wigner symposium*. World Scientific, 1996.
- [3] C. Lipp and C. Jung. From scattering singularities to the partition of a horseshoe. *Chaos*, 9:706, 1999.
- [4] A. Selberg. Harmonic analysis and discontinuous groups in weakly symmetric Riemannian spaces with application to Dirichlet series. *J.Indian Math.Soc.*, 20:47, 1956.
- [5] R. Balian and C. Bloch. Solution of the Schrödinger equation in terms of classical paths. *Ann.Phys.*, 85:514, 1974.
- [6] M. C. Gutzwiller. *Chaos in Classical and Quantum Mechanics*. Interdisciplinary Applied Mathematics. Springer-Verlag, 1990.
- [7] C. Jung and S. Pott. Classical cross section for chaotic potential scattering. *J.Math.A:Math.Gen.*, 22:2925, 1989.
- [8] Carl Störmer. *The polar aurora*. Oxford university press, 1955.
- [9] A. J. Dragt and J. M. Finn. Insolubility of trapped particle motion in a magnetic dipole field. *J.Geophys.Res.*, 81:2327, 1976.
- [10] B. Rückerl and C. Jung. Hierarchical structure in the chaotic scattering off a magnetic dipole. *J.Math.A:Math.Gen.*, 27:6741, 1994.
- [11] M. A. Almeida, I. C. Moreira, and H. Yoshida. On the non-integrability of the Störmer problem. *J.Phys.A:Math.Gen.*, 25:L227, 1992.
- [12] W. H. Press, S. A. Teukolsky, W. T. Vetterling, and B. P. Flannery. *Numerical Recipes in FORTRAN 77*. Cambridge University Press, 1996.

∞

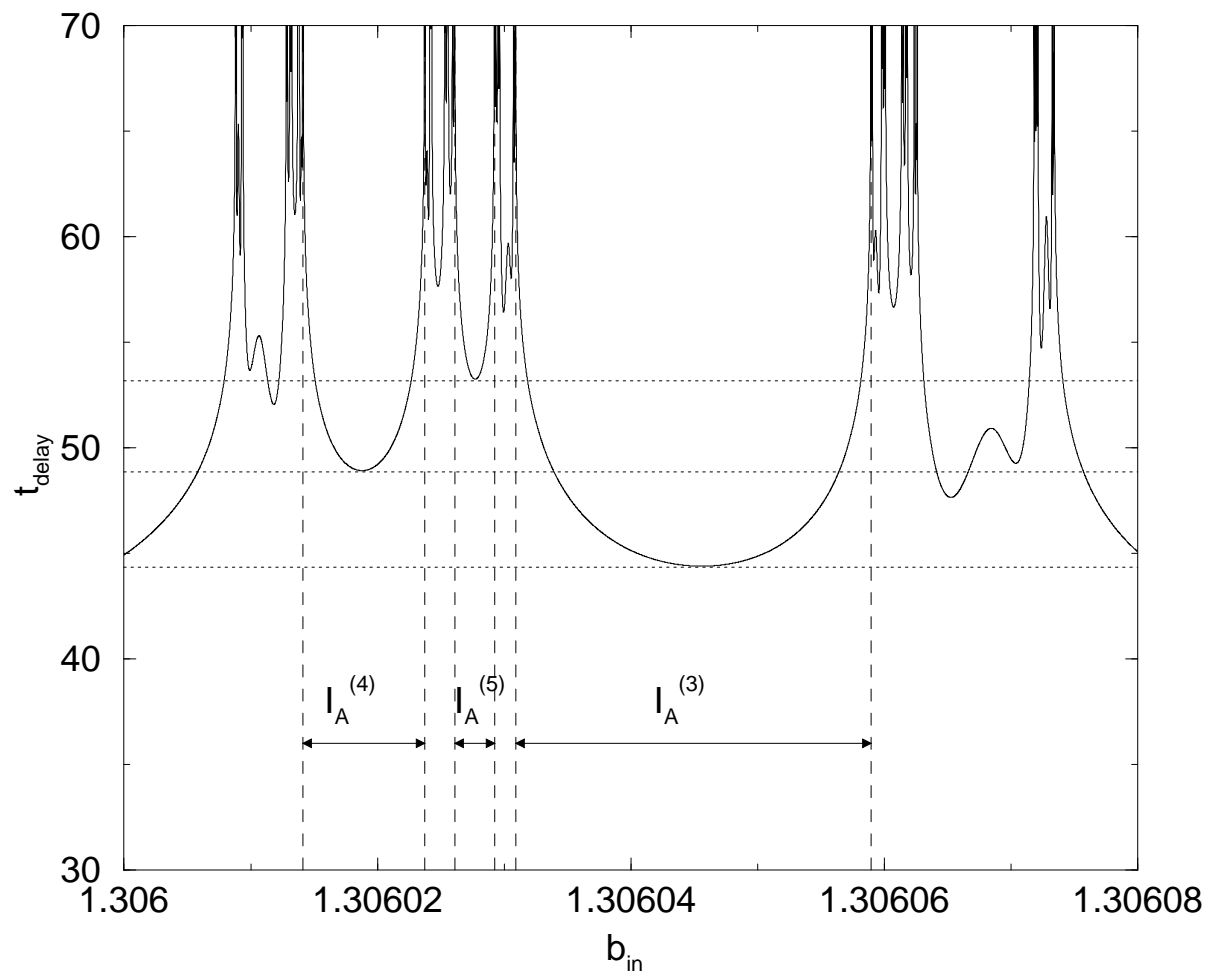


Fig. 1. Time delay function for $\alpha_{\text{in}} = 0$, $E = 0.062$. The consecutive IOC $\{I_A^{(k)}\}_{3 \leq k \leq 5}$ are indicated.

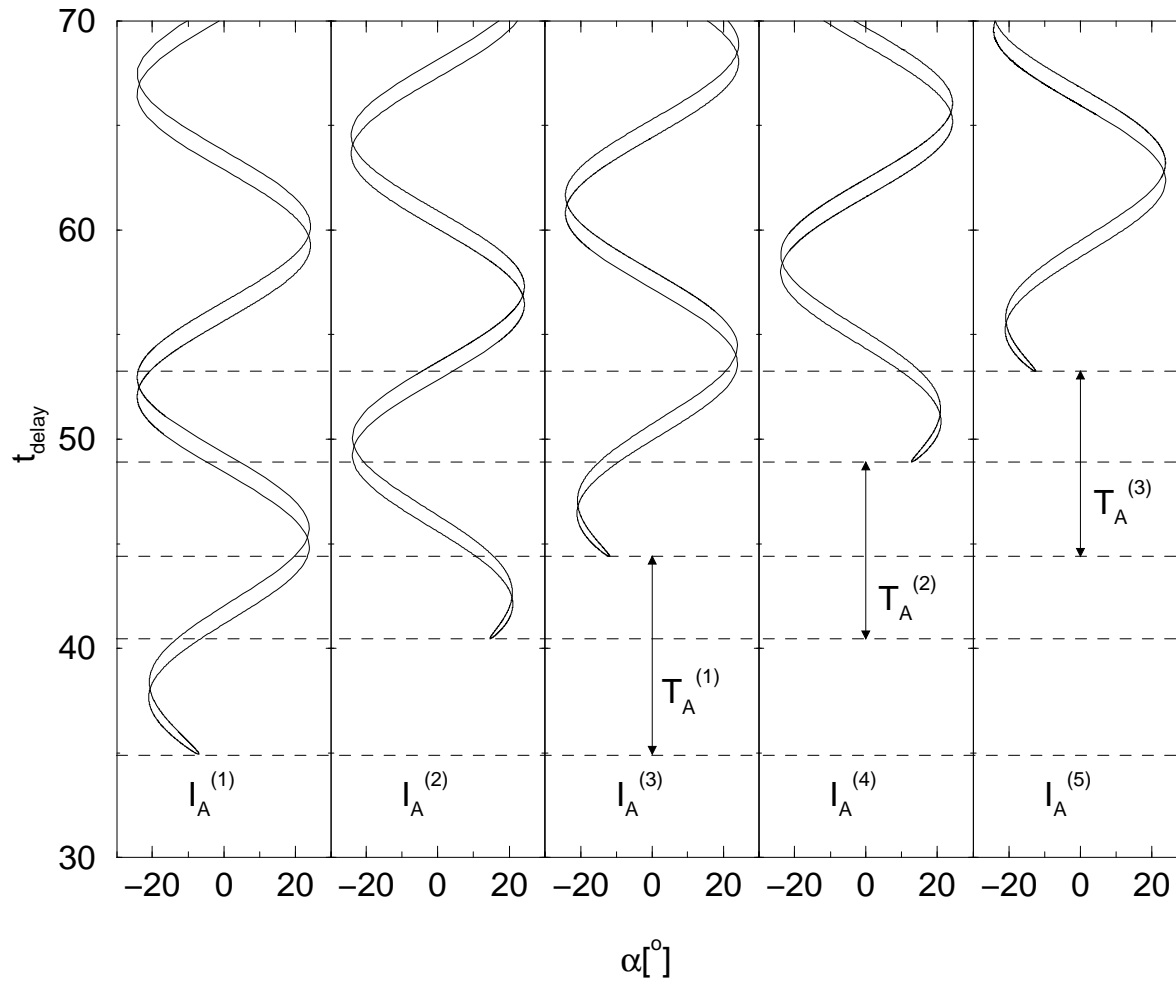


Fig. 2. α_{out} plotted against t_{delay} for the IOC of continuity $I_A^{(1)}, I_A^{(2)}, I_A^{(3)}, I_A^{(4)}, I_A^{(5)}$.

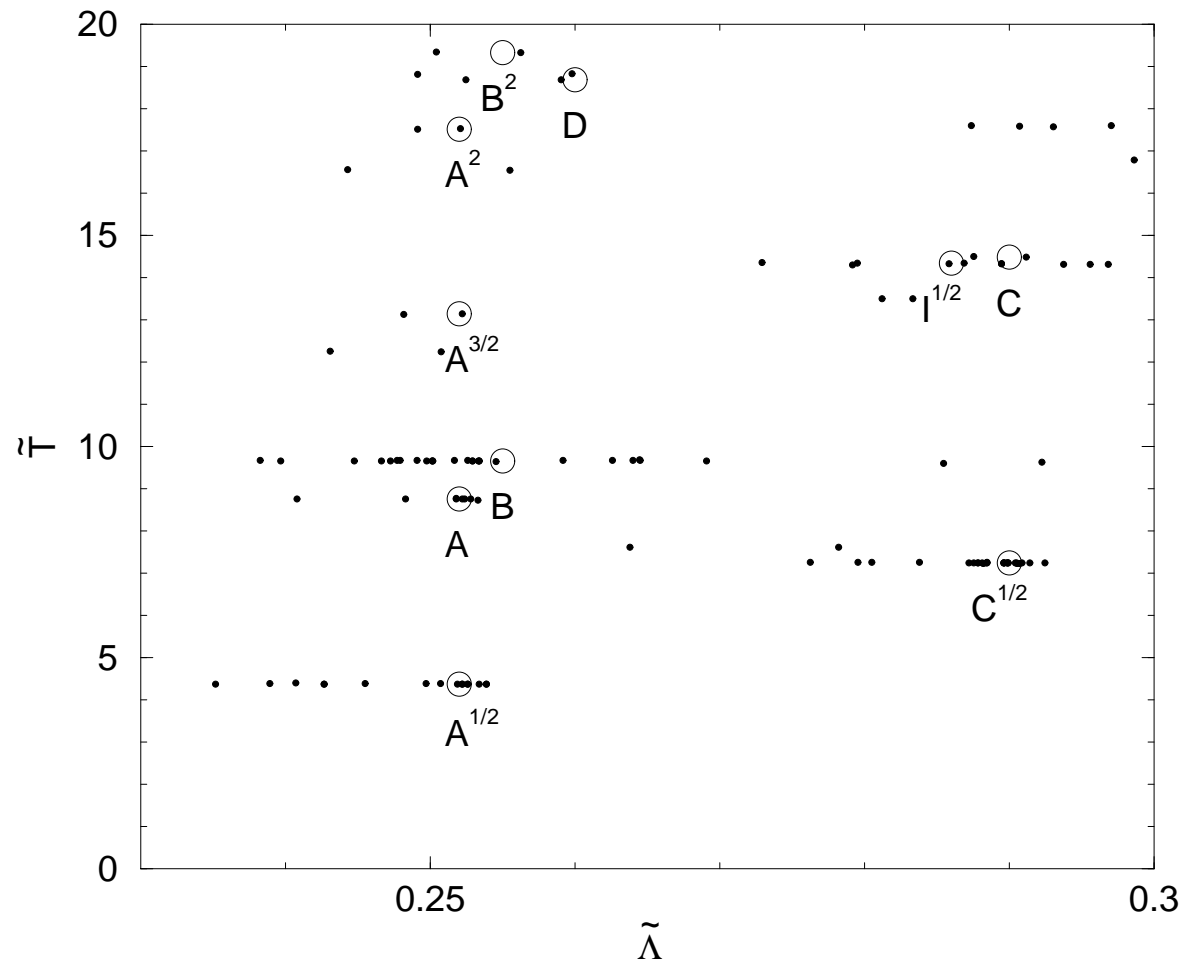


Fig. 3. Periods and Lyapunov exponents of periodic orbits evaluated by only using the time delay function as described in the text. Exact values are marked by open circles and capital letters. The letter's upper indices display what fraction of the full period were measured.

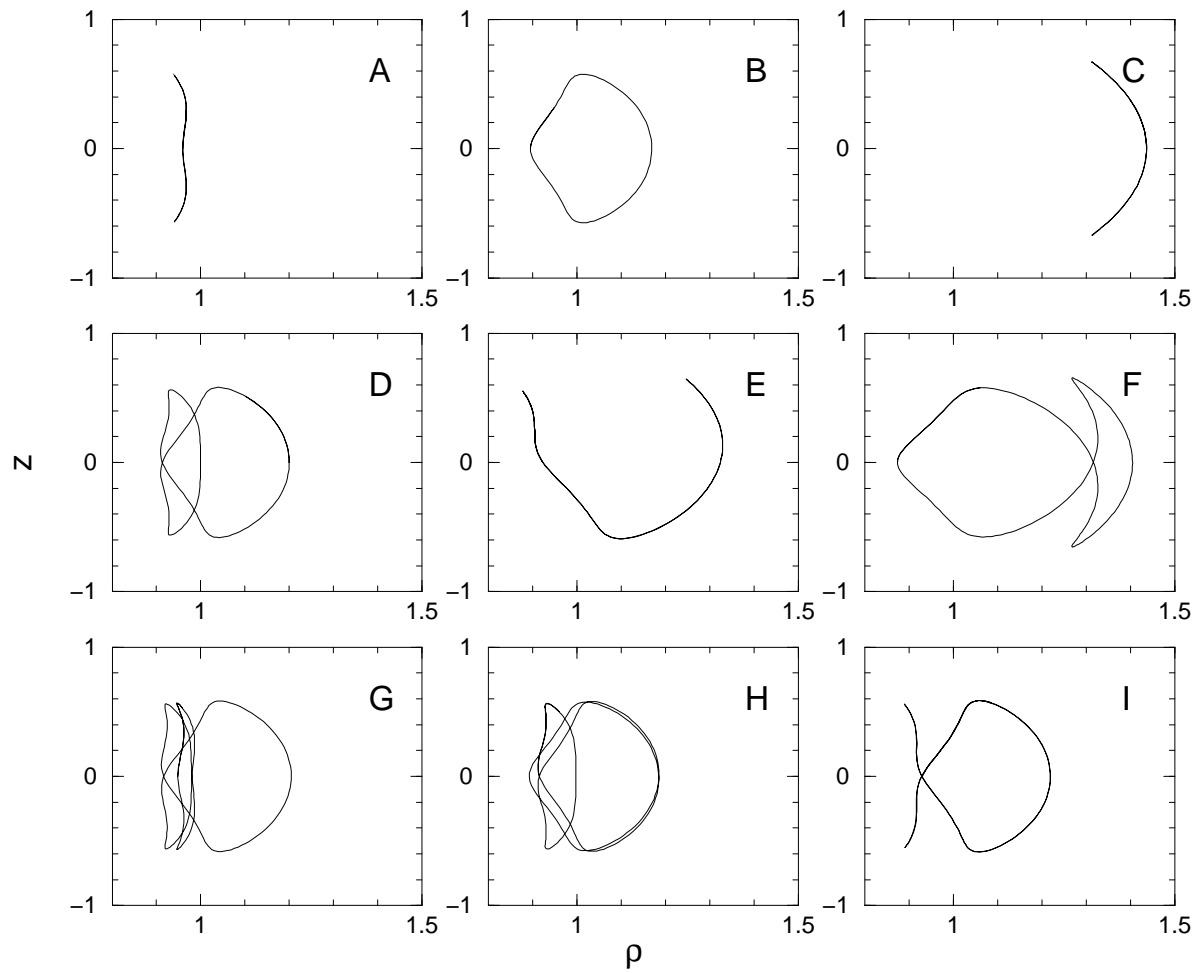


Fig. 4. Projection of periodic orbits in the (ρ, z) -plane.

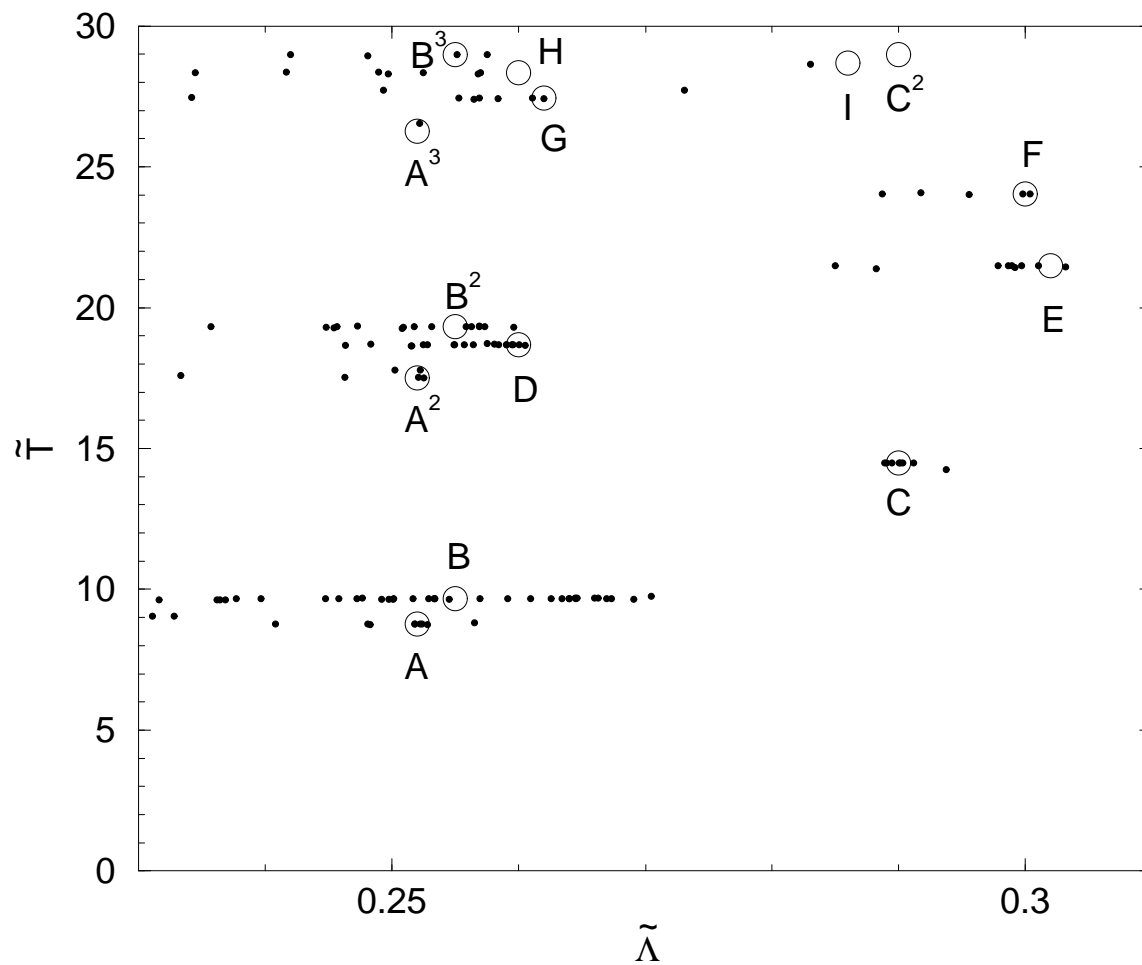


Fig. 5. Periods and Lyapunov exponents of periodic orbits evaluated by using the time delay, α_{out} and b_{out} scattering functions. Exact values are marked by open circles and capital letters. The letter's upper indices display what fraction of the full period were measured.

orbit	#	T_{measured}	T_{exact}	$\Lambda_{\text{measured}}$	Λ_{exact}
A	12	8.762 ± 0.014	8.757	0.245 ± 0.012	0.252
B	41	9.663 ± 0.017	9.661	0.246 ± 0.028	0.255
C	8	14.484 ± 0.005	14.489	0.290 ± 0.001	0.290
D	19	18.678 ± 0.016	18.678	0.253 ± 0.015	0.260
E	4	21.467 ± 0.027	21.485	0.296 ± 0.009	0.302
F	16	24.033 ± 0.016	24.036	0.283 ± 0.023	0.300
G	7	27.450 ± 0.021	27.439	0.254 ± 0.012	0.262
H	6	28.345 ± 0.021	28.333	0.243 ± 0.015	0.260
I	0		28.688		0.286

Table 1

Measured Periods and eigenvalues of periodic orbits. Sample region was $E = 0.062$, $\alpha_{\text{in}} = 0$, $b_{\text{in}} \in [1.3049, 1.3065]$. RMS errors.